Buckling beam micromechanical memory with on-chip readout

D. Roodenburg,[1] J. W. Spronck,[1] H. S. J. van der Zant,[2] and W. J. Venstra[2,a)]
[1]*Precision and Microsystems Engineering, Delft University of Technology, Mekelweg 2, 2628CD Delft, The Netherlands*
[2]*Kavli Institute of Nanoscience, Delft University of Technology, Lorentzweg 1, 2628CJ Delft, The Netherlands*

(Received 19 March 2009; accepted 13 April 2009; published online 4 May 2009)

We have used double clamped beams to implement a mechanical memory. Compressive stress is generated by resistive heating of the beams and beyond the buckling limit the bistable regime is accessed. Bits are written by applying lateral electrostatic forces. The state of the beam is read out by measuring the capacitance between beam and electrodes. Two ways to implement a mechanical memory are discussed: compensation of initial beam imperfections and snap through of the postbuckled beam. Although significant relaxation effects are observed, both methods prove reliable over thousands of write cycles. © *2009 American Institute of Physics*. [DOI: 10.1063/1.3129195]

Bistable micro- and nanomechanical double clamped beam resonators have attracted interest recently in mechanical memory devices[1,2] and sensitive measurement systems.[3] An alternative way to realize a bistable system, avoiding the dissipation associated with resonant devices, is by static axial compression of the double clamped beam.[4] Mechanical memory application of such devices has been proposed, where a microscope is used to read out the beam position.[5,6] In this work we describe a static mechanical memory with a fully electronic interface. On-chip readout enables the integration of the micromechanical bit in electronic or mechanical circuits. Both the compressive and the lateral forces on the beam can be controlled, which allows detailed study and manipulation of the beam behavior. By measurement of the beam position as a function of these forces, we quantify the residual asymmetry in the beam and demonstrate the presence of mechanical relaxation effects, which significantly affect the first few hundred operating cycles of the bit. Two realizations of a micromechanical memory are demonstrated: compensation of beam asymmetry in the prebuckling phase and forced snap through of the postbuckled beam by electrostatic forces. In contrast to mechanical memory based on electrostatic pull in of single clamped cantilever beams,[7,8] the presented memory is contactless and thus less sensitive to wear.

Double clamped beams are fabricated in silicon-on-insulator wafers by optical lithography, followed by reactive ion etching. The beam dimensions are $1000\times6\times35$ μm^3. As the beam height is much larger than its width, the lateral stiffness is low. The beams are released by etching the 2 μm thick silicon oxide insulator layer in a buffered hydrofluoric acid solution. This method yields single-crystal beams with minimal asymmetry and low residual stress. A 600 nm layer of aluminum is sputtered on top to provide a conducting path. Figure 1(a) shows a fabricated and bonded device.

Figure 1(b) schematically shows the setup. Six electrodes are placed around the beam. The beam position is determined by a differential capacitance measurement between the beam and the central electrodes on either side. A pulse excitation signal is therefore applied to the beam. The differential capacitance, ΔC, is measured via an integrated capacitance to digital interface,[9] denoted with C2D in Fig. 1(b). Electrostatic forces are applied to the beam by the four remaining electrodes.

To access the bistable regime, compressive stress is generated by resistive heating of the double clamped beam.[10,11] A constant current is obtained by the driving voltage V_D and the series resistor ($R=175$ Ω) which is large compared to the beam resistance $R_{beam}=7.5$ Ω. The excitation signal, EXC, for the capacitance measurement is added to this driving signal. With no voltages applied to the side electrodes, the curve marked I in Fig. 2(a) shows the measured capacitance as a function of the applied current squared. At $I^2 \approx 2.3\times10^{-3}$ A^2, a gradual transition to the postbuckling phase is initiated. Imperfections in the beam are large enough to prevent bifurcation at the critical beam compression: the beam always buckles in one direction.

When applying voltages to electrodes on one side, the electrostatic force can put the prestressed beam in the other stable position. As Fig. 2(a) shows, different trajectories can be mapped out. The corresponding control voltages V_1 are shown in the inset. Trajectory II is followed when a small electrostatic force is applied to compensate the beam imperfections in the prebuckling regime. Alternatively, a larger electrostatic force may be used to switch the beam in the postbuckling regime of region I, by a forced snap-through.[12]

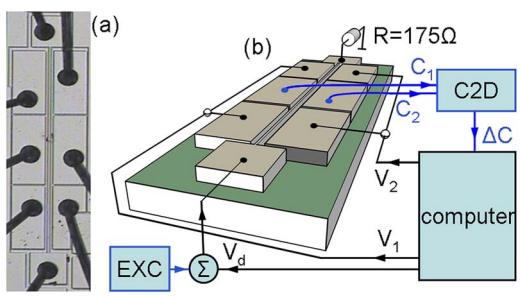

FIG. 1. (Color online) (a) Optical photograph of a fabricated and bonded device. The gap between electrodes and beam is 15 μm. (b) Schematic measurement setup. The beam position is measured using the central electrodes. Lateral forces are applied using the outer electrodes, two of which are present on either side.

a)Electronic mail: w.j.venstra@tudelft.nl.

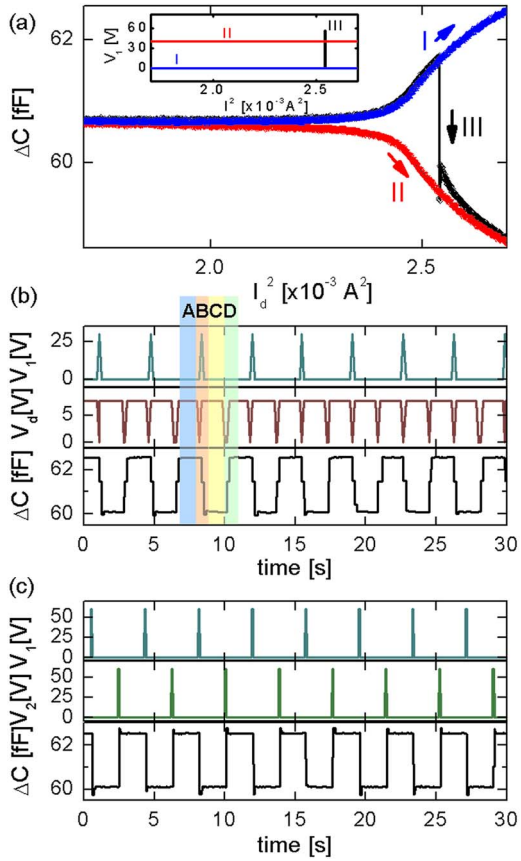

FIG. 2. (Color online) (a) Measured differential capacitance as a function of squared beam current. The inset shows the voltage V_1 corresponding to the three situations in the main figure. (b) Implementation of a mechanical bit based on compensation of imperfections, by following I and II in (a). (c) Implementation of a mechanical bit based on snap-through, by following path III in (a) with the same device.

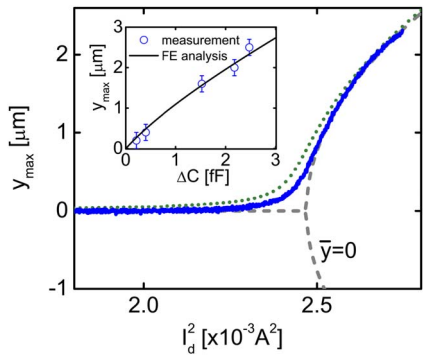

FIG. 3. (Color online) Calibrated beam displacement (solid curve) corresponding to the upper trace in Fig. 2(a), and theoretical curves for an idealized beam [Eq. (1), $\bar{y}=0$; dashed] and a beam with an initial mode amplitude of $\bar{y}=10$ nm (dots). Inset: measured and calculated relation between the beam displacement y_{max} and the differential capacitance ΔC.

This trajectory is shown in trace III, where the initial trajectory coincides with trace I.

As both stable states are accessible, the beam can function as a mechanical memory. Mechanical bit operations via trajectories I and II in Fig. 2(a) are demonstrated in Fig. 2(b). The two upper panels show the electrostatic voltage V_1 and the drive voltage V_d that heats and buckles the beam. The measured capacitance, shown in the lower panel, represents the content of the bit. The beam position corresponding to a low capacitance represents a logical "0." Depending on the control voltages, either high or low, the bit is set and reset. The sequence ABCD represents the write operations. During stage A, a logical "1" is memorized. The beam is compressed and remains in its "high" position. In stage B, the beam current is low and a voltage is temporarily applied to the side electrode to compensate the asymmetry of the beam. After reapplying the current, the beam buckles to the "low" position, which represents a logical "0." This value is memorized during stage C, while the electrostatic force is zero. In stage D, the beam is reset to its preferred buckling position by setting the driving current temporarily low. This corresponds to the initial situation, a logical "1."

In an alternative implementation, the beam remains compressed and is switched between the postbuckled states, following trajectory III in Fig. 2(a). Figure 2(c) shows the operation. The upper panels show the control electrostatic voltages V_1 and V_2, which are 50 ms pulses. A higher voltage is required to switch between postbuckling states than in panel (b). This scheme requires electrodes on both sides of the beam as to set and reset the beam position. Similar to Fig. 2(b), the pulse sequences clearly demonstrate the controlled writing and erasing of the bit.

We will now analyze the results in more detail, and for this, the changes in differential capacitance have to be related to the beam displacement. A calibration was carried out by measuring the differential capacitance as a function of the displacement of the beam center, using a scanning optical microscope.[13] The inset in Fig. 3 shows the result. The relation between differential capacitance and the displacement of the beam is approximately 1 μm/fF. A finite element analysis confirms this value for displacements up to a few micrometers.

To calculate the compressive stress, the average temperature of the beam as a function of the applied current is calculated by solving Fourier's law of heat conduction. Convection and radiative heat transport are neglected, which is a valid assumption for our device dimensions.[4] Taking into account the conduction through the beam clamping points, and the conduction through the air film between the beam and the substrate as a fit parameter, the relation between driving current and induced stress due to a change in the average beam temperature equal to ΔT_{avg} can be approximated by $\epsilon = \alpha \Delta T_{avg} \approx 1.8 \times 10^4 \times I_d^2$. The thermal expansion, α, is assumed constant within the temperature range in the experiments ($\Delta T \approx 60$ K). As a result of the stress, the displacement of the beam center is calculated by the real part of

$$y_{max} = \pm \sqrt{\frac{4}{3}\left(\frac{\epsilon}{\epsilon_1} - 1\right)d^2}, \tag{1}$$

where for a beam with rectangular cross section the critical compression for mode 1 equals $\epsilon_1 = -(\pi^2 d^2 / 3L^2)$, where L is the length and d is the width of the beam. Equation (1) corresponds to the dashed curve in Fig. 3.

The minimum energy to switch the beam is related to imperfections in the beam. These imperfections can be taken into account by assuming an initial curvature $\bar{y}$, which is supposed to take the shape of the first static mode.[14] Including this term, the potential energy in the compressed double clamped beam is calculated as[15]

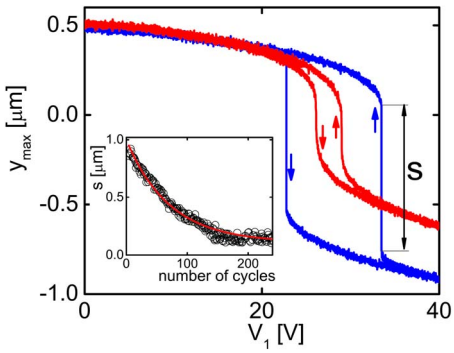

FIG. 4. (Color online) Center beam displacement while sweeping V_1 forth and back. The sweep direction is indicated by the arrows. The blue trace represents the initial cycle. The red trace shows one measurement after 210 repetitions. The inset shows the measured reduction of the flight distance, s, as a function of the number of cycles. The red line represents an exponential fit through the data.

$$U(y) = \frac{EI_z L k_1^4}{16}(y-\bar{y})^2 + \frac{EALy^2}{16}k_1^2\left(\epsilon + \frac{k_1^2 y^2}{32}\right), \qquad (2)$$

where E is Young's modulus, and $k_1 = 2\pi/L$. We calculated the static mode amplitude as a function of the beam current and plotted the results together with an ideal beam and the calibrated displacement of the solid line in Fig. 2(a) in Fig. 3. The model reproduces the beam displacement including the point of buckling well. The predefined buckling direction can then be related to an initial curvature on the order of 10 nm. Although our fabrication process yields beams with little asymmetry compared to silicon oxide beams with high residual stress and similar L/d ratio,[15] asymmetries due to imperfect fabrication are still two orders of magnitude larger than the beam movements by thermal fluctuations.

The reliability of the mechanical memory was investigated by repeating the measurements shown in Figs. 2(b) and 2(c) thousands of times. During these experiments, we observed significant relaxation effects in the double clamped beams. These effects were investigated as follows. We first prestressed the beam at $I_d^2 = 2.46 \times 10^{-3}$ A^2 and then measured the beam position while slowly attracting the beam through the instable region. Figure 4 shows the measured displacement as a function of the electrostatic force induced by V_1. The first loop represented by the blue curve shows a large hysteresis. The flight distance is indicated by s. The red trace shows the curve measured after 210 repetitions. A clear reduction of the hysteretic area is observed, and s has decreased by a factor 4. The inset in Fig. 4 shows s versus the number of cycles during this experiment. The flight distance initially drops very fast, and eventually saturates at a fraction of its initial value. We note that the memory function is not lost, as s has not reduced to zero. The measurements fit an exponential decay reasonably well, as shown by the red line. Similar behavior was observed in several other devices, and by varying the sweep time of V_1 we verified that the independent variable is the number of cycles, rather than the time to sweep V_1.

The exponential reduction of the displacement with the number of switches indicates a mechanical relaxation effect, acting on the initial shape of the beam. A likely mechanism is the nucleation and/or evolution of dislocations at the compressed side of the silicon beam,[16] which can lead to a significant reduction in the deflection of buckled beams.[17] These irreversible processes result in a reduction of the flight distance to a stable value. Using a high-resolution optical microscope, we qualitatively observed changes in the beam shape before and after repetitive switching. The observed effects may lead to a reduction in the signal to noise ratio, and to small changes in the threshold voltages. However, at large driving currents, both bit operations were found to be reliable over thousands of cycles.

To decrease the footprint area of the mechanical bit, we experimented with 79 μm long beams, with gaps between electrodes and beams equal to 5 μm, and found that the capacitive displacement detection with the presented setup is still feasible. We note that capacitance detection has been proven a viable way to detect displacements in double clamped beams with dimensions a factor 10^3 smaller than the ones presented here,[2] which suggests scalability down to such dimensions. Finally, we note that in the scheme of Fig. 2(c), compressive stress can be introduced during fabrication, as to eliminate the need for current while the bit is memorized.[6]

In summary, we demonstrated a micromechanical static memory device based on a buckling beam, with a fully electronic interface. A quantitative analysis of the beam behavior is presented, including the residual beam asymmetries. During the first few hundred operating cycles of the memory we found relaxation effects in the beam. After this "burn-in" period, the memory performance is stable.

The authors acknowledge financial support from FOM and NWO (VICI).

[1] I. Mahboob and H. Yamaguchi, Nat. Nanotechnol. **3**, 275 (2008).
[2] D. N. Guerra, M. Imboden, and P. Mohanty, Appl. Phys. Lett. **93**, 033515 (2008).
[3] R. L. Badzey and P. Mohanty, Nature (London) **437**, 995 (2005).
[4] M. T. A. Saif, J. Microelectromech. Syst. **9**, 157 (2000).
[5] B. Hälg, IEEE Trans. Electron Devices **37**, 2230 (1990).
[6] B. Charlot, W. Sun, K. Yamashita, H. Fujita, and H. Toshiyoshi, J. Micromech. Microeng. **18**, 045005 (2008).
[7] M. A. Beunder, R. van Kampen, D. Lacey, M. Renault, and C. G. Smith, *Sixth Annual Non-Volatile Memory Technology Symposium* (IEEE, New York, NY, 2005), pp. 65–68.
[8] C. G. Smith, R. van Kampen, J. Popp, D. Lacy, D. Pinchetti, M. Renault, V. Joshi, and M. A. Beunder, in *Proceedings of the Society of Photo-Optical Instrumentation Engineers (SPIE)*, edited by S. Tadigadapa, R. Ghodssi, and A. Henning (SPIE, Bellingham, WA, 2007), Vol. 6464, p. 46406.
[9] Analog Devices AD7746 capacitance to digital converter.
[10] U. Lindberg, J. Söderkvist, T. Lammerink, and M. Elwenspoek, J. Micromech. Microeng. **3**, 183 (1993).
[11] M. Chiao and L. Lin, J. Microelectromech. Syst. **9**, 146 (2000).
[12] S. Krylov, B. R. Ilic, D. Schreiber, S. Seretensky, and H. Craighead, J. Micromech. Microeng. **18**, 055026 (2008).
[13] Keyence VX-100 optical microscope with lateral scanner.
[14] W. Fang and J. A. Wickert, J. Micromech. Microeng. **4**, 116 (1994).
[15] W. E. Lawrence, M. N. Wybourne, and S. M. Carr, New J. Phys. **8**, 223 (2006).
[16] J. Li, K. J. Van Vliet, T. Zhu, and S. Suresh, Nature (London) **418**, 307 (2002).
[17] J. Durinck, C. Coupeau, J. Colin, and J. Grilhé, Appl. Phys. Lett. **93**, 221904 (2008).